JMBFS
Journal of Microbiology, Biotechnology and Food Sciences
International peer-reviewed scientific online journal
Published by Faculty of Biotechnology and Food Sciences

ISOLATION AND *IN SILICO* STUDIES OF A LACCASE GENE FROM *Trametes hirsuta* EDN 082: STRUCTURAL AND FUNCTIONAL ANALYSIS FOR BIOREMEDIATION OF SYTHETIC DYES

Muhamad Ilham[1], Anja Meryandini[2], Dede Heri Yuli Yanto[3], Asrul Muhamad Fuad[4], Fina Amreta Laksmi[3], Nanik Rahmani[3], Oktan Dwi Nurhayat[3], Takashi Watanabe[5]*

Address(es):
[1] Master program in Biotechnology, Graduate School, IPB University, Dramaga Campus, Bogor 16680, Indonesia.
[2] Department of Biology, Faculty of Mathematics and Natural Sciences, IPB University, Darmaga Campus, Bogor 16680, Indonesia.
[3] Research Center for Applied Microbiology, National Research and Innovation Agency (BRIN), Soekarno Science and Techno Park. Jl. Raya Bogor Km.46, Cibinong, Bogor 16911, Indonesia.
[4] Research Center for Genetic Engineering, National Research and Innovation Agency (BRIN), Soekarno Science and Techno Park. Jl. Raya Bogor Km.46, Cibinong, Bogor 16911, Indonesia.
[5] Research Institute for Sustainable Humanosphere, Kyoto University, Uji Campus, Kyoto 611-0011, Japan.

*Corresponding author: dede.heri.yuli.yanto@brin.go.id

https://doi.org/10.55251/jmbfs.12435

ARTICLE INFO

Received 24. 2. 2025
Revised 13. 1. 2026
Accepted 26. 3. 2026
Published 1. 6. 2026

Regular article

OPEN ACCESS

ABSTRACT

Trametes hirsuta produces multiple laccases capable of decolorizing synthetic dyes. In this study, a thermostable, high-redox-potential extracellular blue laccase gene named *Thlacc1* was successfully isolated from the transcriptome of *T. hirsuta* EDN 082. The *Thlacc1* gene was isolated using the cDNA library construct, followed by PCR using degenerate and specific primers, respectively. The *Thlacc1* gene (1575 bp) encodes a 524-amino acid protein with 98.47% similarity to laccase 3 (AOX15704.1), classifying it within the minor laccase group F. Primary structure analysis on ExPASy ProtParam server predicted a molecular weight of 56.54 kDa, an isoelectric point of 4.88, a stability index of 29.13, an aliphatic index of 97.33, and a GRAVY score of -0.130. Secondary structure analysis highlighted β-strands and helices, while tertiary structure modeling on the SwissModel server presented Model 03 as the most accurate model. The enzyme contains three multicopper oxidase motifs, a signal peptide, four N-glycosylation and nine O-glycosylation sites, four copper-binding domains (L1-L4), two disulfide bonds, and a catalytic pocket (221 Å³). Molecular docking at the T1 copper site using the SwissDock server revealed potential interactions between Model 03 and synthetic dyes. DB71 and RB5 showed the highest (-8.44 kcal/mol) and lowest (-5.825 kcal/mol) binding affinities, respectively, but neither was decolorized experimentally. In contrast, recombinant *Thlacc1* laccase efficiently decolorized AB113 and AB129, indicating that decolorization efficiency depends on both binding affinity and key-interacting residues. This study provides structural insight and experimental validation for the application of *Thlacc1* laccase in the decolorization of synthetic dyes.

Keywords: Laccase; *Trametes hirsuta;* Gene isolation; *In silico* analysis; Synthetic dyes; Decolorization

INTRODUCTION

Synthetic dyes have been widely utilized in the textile industry due to their vibrant and colorfast properties. However, their extensive use poses significant environmental and health risks. Textile effluents, often laden with dyes, chemicals, and heavy metals, can contaminate water bodies, disrupt aquatic ecosystems, and impair photosynthetic processes **(Al-Tohamy *et al*., 2022).** Alarmingly, around 280,000 tons of untreated textile dyes are released into the environment annually **(Jorge *et al*., 2023)**. Untreated textile dyes pose significant environmental and health risks due to their persistence and toxicity **(Hoque *et al*., 2024).** Given these risks, textile dye wastewater treatment remains an important issue that needs to be addressed **(Holkar *et al*., 2016).** Various treatment approaches have been developed to mitigate the environmental impact of dye pollution, including physical, chemical, and biological methods **(Yaseen and Scholz, 2019)**. However, the persistence and complexity of synthetic dyes necessitate more effective and sustainable solutions.

Bioremediation of synthetic dyes from textile effluents using biological methods has gained attention as an eco-friendly alternative to conventional treatments **(Sudarshan *et al*., 2022)**. The use of microorganisms has shown significant potential for the degradation and decolorization of synthetic dyes **(Panwar *et al*., 2023)**. These biological methods offer cost-effective and environmentally friendly alternatives to conventional physicochemical treatments. Microbial degradation of dye molecules involves enzymatic processes, utilizing enzymes such as peroxidase, laccase, and azoreductase **(Das *et al*., 2023)**.

Laccase (EC 1.10.3.2) belongs to a group of enzymes in the multicopper oxidase (MCO) family, distinguished by the presence of multiple copper (Cu) atoms and classified as benzenediol oxygen reductases **(Giardina *et al*., 2010)**. These enzymes have broad substrate specificity, allowing them to oxidize a diverse range of phenolic and non-phenolic compounds. Laccases utilize oxygen as an electron acceptor and produce water as a byproduct **(Kim et al., 2001; Morozova et al., 2007)**; therefore, they are widely employed as green catalysts in the bioremediation of synthetic dyes. Laccases are classified into three main types: blue, white, and yellow, based on their copper content and absorption spectra **(Sondhi *et al*., 2023)**. Blue laccases exhibit a characteristic absorption peak at 605 nm, due to their Type I copper atom, while white and yellow laccases lack this peak but show absorption at 400 nm **(Agrawal and Verma, 2020)**. Additionally, laccases are classified based on the redox potential (E°) of the Type I (T1) copper site. The redox potential at this location varies among enzymes, typically falling within the range of 0.4 to 0.8 V relative to the normal hydrogen electrode (NHE). Based on these values, laccases are categorized into low (0.4-0.5 V), medium (0.5-0.6 V), and high (0.7-0.8 V) redox potential categories **(Mate and Alcalde, 2015)**. Laccases from various organisms, including fungi, bacteria, plants, and invertebrates, have been obtained and utilized to meet the growing industrial demands **(Cardullo *et al*., 2022)**.

Fungal laccases are versatile enzymes with significant potential in bioremediation applications. These blue multicopper oxidases are primarily secreted by white-rot and litter-decomposing fungi **(Viswanath *et al*., 2014)**. This particular group of fungi is known to produce laccases with the ability to degrade pesticides such as dichlorodiphenyltrichloroethane (DDT) in soil **(Zhao *et al*., 2010)** and PAHs, including anthracene, fluoranthene, fluorene, perylene, phenanthrene, and pyrene, when assisted by synthetic mediators **(Pozdnyakova *et al*., 2006)**. The laccases produced by white-rot fungi are also able to catalyze the bioremediation of phenolic compounds, bisphenol A, naproxen, alkylphenols, and synthetic dyes **(Barrios-Estrada *et al*., 2018; Marco-Urrea *et al*., 2010; Farnet *et al*., 2000; Yanto *et al*., 2019)**.

Various fungal sources, such as *Aspergillus oryzae, Trametes versicolor*, *Paraconiothyrium variabile*, and *Trametes hirsuta,* have been studied for laccase production and dye decolorization **(Forootanfar *et al*., 2012; Yanto *et al*., 2022)**.

The efficiency of dye decolorization is varied and could be improved through the use of mediators, though it varies depending on the dye type and enzyme source. Laccase mediators, such as hydroxybenzotriazole (HBT) and violuric acid (VA), can significantly enhance decolorization efficiency **(Forootanfar *et al.*, 2012; Yanto *et al.*, 2019)**. The immobilization of laccase has also been shown to enhance dye decolorization compared to the free enzyme **(Ali *et al.*, 2019)**. Laccase-mediated bioremediation of synthetic dyes has been shown to generate byproducts with reduced toxicity, highlighting its potential for wastewater treatment (**Yanto *et al.*, 2019).**

Basidiomycete fungi are the most common and preferred sources of laccases, particularly blue laccase, due to their higher oxidation potential compared to other organisms **(Mate and Alcalde, 2015)**. *Trametes hirsuta* is a white-rot fungus from the basidiomycete group that has emerged as a promising source of laccase. Specifically, *T. hirsuta* 072 produces several functional laccase isoenzymes, classified into group A-G based on gene sequence homology **(Savinova *et al.*, 2019)**. *T. hirsuta* EDN 082 (GenBank: MT476912.1) produces native laccases with decolorization activity against various dyes, including Remazol Brilliant Blue R, anthraquinone, and azo dyes **(Anita *et al.*, 2020; Yanto *et al.*, 2022)**. Furthermore, *T. hirsuta* EDN 082 exhibits biodegradation and detoxification activity in batik dye wastewater, making it a valuable candidate for bioremediation **(Yanto *et al.*, 2021)**. However, the genetic basis for these enzymatic activities remains poorly understood, particularly with respect to the specific laccase gene responsible for these properties. Thus, isolating and characterizing the laccase-encoding gene from *T. hirsuta* EDN 082 is crucial for understanding its functional potential and optimizing its future applications in bioremediation.

In silico approaches have emerged as powerful tools for improving enzyme catalytic properties and thermal stability. Computational methods, including bioinformatics, molecular modeling, and de novo design, can be combined to enhance enzyme performance **(Damborsky and Brezovsky, 2014)**. These methods can guide experimental planning, rationalize resources, and provide insights into protein-substrate interactions **(Ebert and Pelletier, 2017)**. They offer precise guidance for enzyme modification, making the process more efficient and less laborious **(Li *et al.*, 2012)**. *In silico* studies typically involve characterizing physicochemical properties, predicting secondary and tertiary structures, identifying functional domains and motifs, and conducting phylogenetic analyses **(Nene *et al.*, 2022; Dutta *et al.*, 2018)**. In the present study, a gene encoding the laccase enzyme has been isolated from the transcriptome of T. hirsuta EDN 082 and characterized through in silico studies to understand its structural and functional properties, as well as its potential as a catalyst in the bioremediation of synthetic dyes.

MATERIAL AND METHODS

All chemicals used in this research are of the highest purity available. The gene source, *Trametes hirsuta* EDN 082 (GenBank ID: MT476912.1), was obtained from the isolate collection of the Microbial Composite Engineering Research Group at the National Research and Innovation Agency (BRIN), Indonesia.

Total RNA Extraction and cDNA Synthesis

Trametes hirsuta EDN 082 was grown in Malt Extract Broth (Himedia, India) supplemented with 50 g/L oil palm empty fruit bunch (OPEFB) at pH 6.0. Cultures were incubated at 27 °C with shaking at 100 rpm for seven days.

A total of 100 mg of biomass was collected for RNA extraction using the Direct-Zol™ RNA Miniprep Kit with TRI Reagent (Zymo Research, USA), following the manufacturer's protocol. RNA concentration and purity (A260/A280 > 1.8) were measured with a Nanodrop.

Complementary DNA (cDNA) was synthesized using the ReverTra Ace™ qPCR RT Master Mix with gDNA Remover (TOYOBO, Japan). PCR verification was performed using ITS5F (5′-TCCGTAGGTGAACCTGCGG-3′) and reverse primer ITS4R (5′-TCCTCCGCTTATTGATATGC-3′), and amplification products were visualized on a 1% agarose gel.

Laccase Gene Exploration and Full Gene Amplification

Degenerate Primer Design. Degenerate primers were designed based on seven T. hirsuta 072 laccase genes (laccase A-G, GenBank KP027478.1, KP027484.2, KP027479.1, KP027480.1, KP027481.1, KP027482.1, and KP027483.1). Multiple sequence alignment in BioEdit 7.0 (**Hall, 1999**) identified four conserved regions used for primer design (Supplementary Figure S1). Primer sequences and predicted product lengths are listed in Supplementary Table S1.

Partial Gene Amplification. PCR was performed in 10 µL reactions containing 2× MyTaq HS Red Mix, primers, and cDNA. Cycling conditions included denaturation (95 °C), annealing (50-52 °C, respectively), and extension (72°C), followed by agarose gel electrophoresis. Sequenced fragments were analyzed using BLASTn to identify target genes for the design of specific primers.

*Full-Length Gene Amplification***.** Specific primers (Supplementary Table S2) were used for full ORF amplification. PCR conditions included denaturation (95°C), annealing (56-60 °C, respectively), and extension (72 °C). Optimized conditions yielded single, distinct bands. The products were purified and sequenced using Sanger sequencing.

Primary Sequence Analysis on Putative Laccase Gene

Sanger sequencing data (.ab1 files) were processed in Benchling (https://benchling.com/). Poor-quality chromatogram regions were trimmed, and high-quality reads were assembled into a single nucleotide sequence. Open reading frames were identified using NCBI ORF Finder (https://www.ncbi.nlm.nih.gov/orffinder/), and amino acid sequences were derived. Codon usage was analyzed with the Codon Usage tool (https://www.bioinformatics.org/sms2/codon_usage.html), and GC content was calculated in Benchling. Homology searches were performed using BLASTp (https://blast.ncbi.nlm.nih.gov/Blast.cgi).

Phylogenetic analysis was conducted using MEGA X (Kumar et al., 2018) with the maximum-likelihood algorithm and 1000 bootstrap replications to generate the phylogenetic tree. The physicochemical properties of the amino acid sequence, such as composition, molecular weight, instability index, isoelectric point (pI), extinction coefficient, aliphatic index, and grand average of hydrophobicity (GRAVY), were assessed using the ExPASy ProtParam tool (https://web.expasy.org/protparam/).

Secondary Structure Prediction

Polyview2D (https://polyview.cchmc.org/) was used to predict the secondary structure and its elements. At the same time, PDBsum (http://www.ebi.ac.uk/thornton-srv/databases/pdbsum/) was utilized to derive the secondary structure and determine the percentage composition of structural elements from a validated 3D model.

Tertiary Structure Prediction and Validation

Homology models were generated using SwissModel (https://swissmodel.expasy.org/). The model quality was assessed using SwissModel Structure Assessment (https://swissmodel.expasy.org/assess), ProSA (Z-score at https://www.came.sbg.ac.at/prosa.php), ERRAT, and Verify3D at https://saves.mbi.ucla.edu/, and QMEAN at https://swissmodel.expasy.org/qmean/ to obtain the validity of models based on their closeness to the experimentally determined tertiary structure in the database.

Functional Analysis

InterProScan (https://www.ebi.ac.uk/interpro/search/sequence/) identified functional domains, families, and motifs. PROSITE (https://prosite.expasy.org/) detected signature motifs, and SignalP 6.0 (https://services.healthtech.dtu.dk/services/SignalP-6.0/) predicted signal peptides. Glycosylation sites were predicted with NetNGlyc-1.0 (https://services.healthtech.dtu.dk/services/NetNGlyc-1.0/) and NetOGlyc-4.0 (https://services.healthtech.dtu.dk/services/NetOGlyc-4.0/) servers, respectively. Multiple sequence alignment (https://www.ncbi.nlm.nih.gov/tools/cobalt/re_cobalt.cgi) with other *T. hirsuta* laccases identified conserved cysteines and copper-binding motifs. Disulfide bonds were visualized in ChimeraX 1.8 **(Meng *et al.*, 2023)**, thermal stability was predicted with SCooP (http://babylone.3bio.ulb.ac.be/SCooP/index.php), and the substrate-binding cavity was identified using CB-DOCK2 (https://cadd.labshare.cn/cb-dock2/index.php),

Molecular Docking of Laccase to Synthetic Dyes

Protein Structure Preparation. The validated 3D model was prepared in ChimeraX 1.8.

Ligand Preparation. The Simplified Molecular Input Line Entry System (SMILES) identifiers for each ligand (2,2'-Azino-bis(3-ethylbenzothiazoline-6-sulfonic) acid (ABTS), Remazol Brilliant Blue R (RBBR), Indigosol, Anthraquinone, Acid Blue 129 (AB129), Acid Blue 113 (AB113), Reactive Blue 4 (RB4), Reactive Black 5 (RB5), and Direct Blue 71 (DB71)) were obtained from the PubChem database (https://pubchem.ncbi.nlm.nih.gov/).

Molecular Docking. Molecular docking was performed using the "Docking with AutoDock Vina" feature on the SwissDock server (https://www.swissdock.ch/) to obtain 20 receptor-ligand poses.

Visualization and Analysis. The best-scoring poses were visualized in ChimeraX 1.8, and 2D interaction diagrams were created using BioVia Discovery Studio (https://discover.3ds.com/discovery-studio-visualizer-download).

Experimental Validation of Decolorization Activity of Laccase to Synthetic Dyes

The recombinant laccase was obtained from a previous study by Ilham (2025), in which the corresponding laccase gene was heterologously integrated into the genome of *Pichia pastoris* at the AOX1 promoter. The recombinant protein was

harvested after 3 days of cultivation under methanol induction, followed by ammonium precipitation and purification using a His-Spin protein miniprep kit (Zymo Research, USA). The pure enzyme was then tested against selected dyes, namely Acid Blue 129 (AB129), Acid Blue 113 (AB113), Direct Blue 71 (DB71), and Reactive Black 5 (RB5). All selected dyes were of the highest purity available. A series of experiments using 0.2 U/mL of pure recombinant laccase was conducted with 50 ppm of synthetic dyes, respectively. The samples were then incubated for 3 hours at room temperature with 1-hour intervals for measurements. The experiment conditions and equation used to measure the decolorization rate follow the previous study by **Anita *et al.* (2020)**. All experiments were done in triplicate.

RESULTS

Total RNA Extraction and cDNA Synthesis

A previous study by **Yanto *et al.* (2021)** demonstrated that *T. hirsuta* EDN 082 could produce laccase using oil palm empty fruit bunch (OPEFB) as a lignocellulosic source in the growth medium. Similarly, **Vasina *et al.* (2016)** reported that transcription of laccase-encoding genes in *T. hirsuta* 072 began as early as three days post-incubation in GP-salt medium supplemented with a lignocellulosic source.

In the present study, a Malt Extract Broth medium supplemented with OPEFB was used to maximize the transcription of laccase-encoding genes in *T. hirsuta* EDN 082, thereby increasing the mRNA copy number of the laccase gene. Total RNA isolated from *T. hirsuta* EDN 082 yielded RNA concentrations of 74 ng/µL (A260/280 = 1.84; A260/230 = 2.391) and 218 ng/µL (A260/280 = 1.83; A260/230 = 2.419) from mycelium samples. The purity of the isolated RNA was assessed and found to be suitable for downstream applications. According to **Jain (2020)**, RNA is considered pure when the A260/A280 ratio is approximately 2.0, with protein contamination indicated if the ratio is <1.85.

The total RNA was used as a template for cDNA synthesis, which was subsequently confirmed via PCR. The presence of DNA bands around 650 bp in all samples (see Supplementary Figure S2) indicated successful amplification. The Internal Transcribed Spacer (ITS) region of ribosomal RNA (rRNA) constitutes a significant portion of the transcriptome, accounting for approximately 90% of total RNA **(Chen and Duan, 2011)**. Successful PCR amplification of the ITS region using cDNA as a template further validated the effectiveness of cDNA synthesis.

Laccase Gene Exploration and Full Gene Amplification

Gene exploration was performed using various combinations of forward and reverse degenerate primers. Potential laccase genes were successfully amplified through PCR (Figure 1a), with the PCR product lengths corresponding to the predictions in Supplementary Table S1. The degenerate primer pair LaccCDG-F1 + LaccABCDEFG-R (targeting laccase C, D, and G) successfully amplified a template, yielding a PCR product of over 750 bp at an optimal annealing temperature of approximately 50°C. The primer pair LaccCDG-F2 + LaccABCDEFG-R (also targeting laccase C, D, and G) produced a slightly larger amplicon, approximately 1.1 kb, with the same optimal annealing temperature of 50 °C. Meanwhile, the primer pair LaccABEF-F + LaccABCDEFG-R (targeting laccase A, B, E, and F) generated a product slightly under 1 kb, with the best annealing temperature at 51 °C.

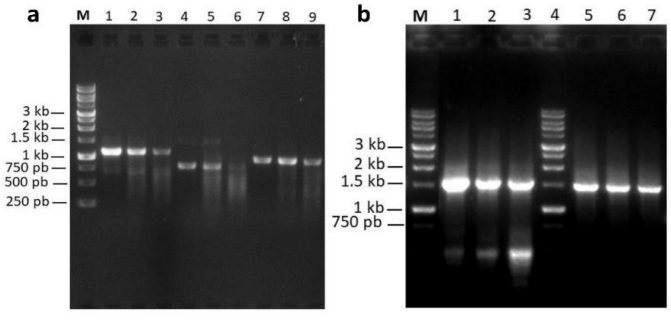

Figure 1 PCR results visualization in Agarose gel 1%; (a) Gene Exploration by PCR using degenerate primer, M: 1 kb DNA Ladder, Lane 1-3: LaccCDG-F2 + LaccABCDEFG-R (annealing at 50 ºC, 51 ºC, and 51 ºC, respectively), Lane 3-6: LaccCDG-F1 + LaccABCDEFG-R (annealing at 50 ºC, 51 ºC, 51 ºC), Lane 7-9: LaccABEF-F + LaccABCDEFG-R (annealing at 50 ºC, 51 ºC, and 51 ºC, respectively), (b) PCR result of full-length laccase genes, M: Marker, lane 1-3: Lacc6_nF+Lacc6_nR (annealing at 56ºC, 58ºC, and 60ºC, respectively), lane 4: Marker, lane 5-7: Lacc3_nF+Lacc3_nR1 (nR1 (annealing at 56ºC, 58ºC, and 60ºC, respectively).

Sequencing results of each PCR product were obtained through Sanger sequencing. The majority of the sequences exhibited multiple background noises, making them unreliable for accurate sequence identification. However, two high-quality readings were obtained: one from LaccCDG-F2 data (131 bp) and another from LaccABCDEFG-R data (242 bp), as shown in Supplementary Table S3. The presence of background noise was likely due to the degenerate nature of the primers, which can amplify multiple template sequences, leading to poor chromatogram quality. This issue could be mitigated by employing computational approaches to optimize primer design and reduce primer degeneracy (**Li *et al.*, 2015**).

BLASTn analysis of both successfully sequenced products showed high similarity to laccase 6 (ON637942.1) from *T. hirsuta* MX2 and laccase 3 (KU878364.1) from *T. hirsuta* T315 (Table S3). These findings suggest that *T. hirsuta* EDN 082 is more closely related to these two strains than to *T. hirsuta* 072, highlighting species divergence that needs further investigation.

PCR using primer combinations targeting both genes resulted in amplicons of similar sizes (Figure 1b), which aligned with *in silico* predictions. The 1.5 kb amplicons, encoding the full-length laccase gene, were optimized at an annealing temperature of 57°C and sequenced to determine the complete gene sequence. Despite successful amplification of both genes, their 93% sequence similarity suggests that they represent the same gene, with notable differences primarily in the signal peptide region. Therefore, the laccase gene 6 (later designated as *Thlacc1*) was selected for further analysis. The sequencing data from three primers (Lacc6-nF, Lacc6-nR, and Lacc6-1105F) were assembled into a single contiguous sequence of 1575 bp (Supplementary Figure S3).

Primary Sequence Analysis of *Thlacc1* Laccase

The sequence obtained from the previous analysis of 1575 bp contained a GC content of 62.41%, encoding 524 amino acids of laccase from *T. hirsuta* EDN 082, with codon usage presented in Supplementary Table S4. This laccase shows high similarities of 98.47% to laccase 3 (AOX15704.1) and 98.09% to laccase 6 (WDI23427.1), as shown in Table 1.

Table 1 BLASTp result of *Thlacc1* laccase

Description	Scientific name	Query cover (%)	Percent identity (%)	Accession number
Laccase 3	*T. hirsuta*	100	98.47	AOX15704.1
Laccase 6	*T. hirsuta*	100	98.09	WDI23427.1
Laccase C	*Trametes sp.* AH28-2	96	98.80	AAW28934.1
Phenoloxidase	*Trametes versicolor*	100	89.12	XP_008036898.1
Laccase F	*T. hirsuta*	100	83.78	AIZ72725.1

Phylogenetic analysis of *Thlacc1* laccase alongside 15 laccases from *T. hirsuta* (Figure 2) produced similar trees when constructed using both nucleotide and amino acid sequences. The phylogenetic trees were divided into four clades, reflecting the evolutionary relationships among these multigenic enzymes. *Thlacc1* grouped within Clade II alongside *T. hirsuta* laccase F (KP027482.1), *T. hirsuta* laccase 6 (ON637942.1), and *T. hirsuta* strain T315 laccase 3 (KU878364.1). These results suggest that *Thlacc1* belongs to the minor laccase group F, consistent with the classification by **Savinova *et al.* (2019)**.

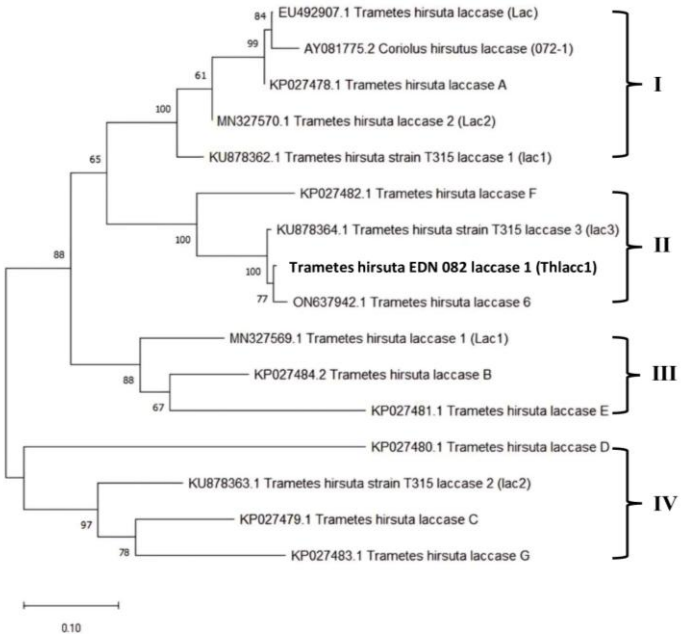

Figure 2 Phylogenetic tree of *Thlacc1* with 15 laccases of *T. hirsuta* available in the gene bank, highlighting the clades within the tree (I-IV)

Analysis of dominant residues (Supplementary Figure S4) identified Alanine (Ala), Threonine (Thr), Glycine (Gly), Leucine (Leu), Aspartate (Asp), Proline (Pro), and Serine (Ser) as the most abundant amino acids, occurring at frequencies of 46, 43, 41, 41, 39, 36, and 33 residues, respectively. Together, these residues accounted for more than 53% of the total sequence. Functional residues, such as Asparagine (Asn), were also present in relatively high numbers (27 residues), whereas Cysteine (Cys) was the least abundant, with only five residues detected.

Table 2 Physical properties of *Thlacc1* laccase

Protein name	Number of amino acids	Molecular weight (Da)	pI	Extinction coef. (M^{-1} cm^{-1})	Instability index	Aliphatic index	Grand average of hydropathicity (GRAVY)
Thlacc1 Laccase	524	56539.20	4.88	66600[a] and 66350[b]	29.13	79.33	-0.130

[a]Assuming all pairs of Cys residues form cystines; [b]Assuming all Cys residues are reduced

The ProtParam tool result summarized the physicochemical properties of *Thlacc1* laccase in Table 2. *Thlacc1* laccase has a molecular weight of 56539.20 Da and an isoelectric point (pI) of 4.88, indicating mild acidity in nature. The extinction coefficients were 66600 and 66350, while an instability index of 29.13 was predicted to be stable under *in vitro* conditions. The high aliphatic index (79.33) implies thermostability of the enzyme, and a negative GRAVY score (-0.130) classifies *Thlacc1* as a soluble globular enzyme **(Magdeldin *et al*., 2012)**.

Secondary Structure Prediction

Secondary structure prediction was performed using Polyview2D and PDBsum tools. The Polyview2D result in Supplementary Figure S5 predicts the elements of the 2D structure along the sequence, including Relative Solvent Accessibility (RSA), physical-chemical properties, and the confidence level of prediction. There were 43 β-strands or bridges, 16 helices, and predominantly coils. It can be inferred from the 2D structure that the β-strands or bridges were mostly found within the low percentage RSA region, suggesting these structures were buried or inaccessible to the solvent.

The result obtained from PDBsum (Figure 3) was derived from a validated 3D structure and presented the secondary structures, including helices and strands, motifs (β-turn, γ-turn, and β-sheet), disulfide bonds, and residues in contact with copper atoms. In summary, 2D structures consisted of Strand with 175 residues (35.1%), α-helix 26 residues (5.2%), 3-10 helix 20 residues (4%), and other structures 278 residues (55%). There were two disulfide bonds and eight beta turns within the 2D structure.

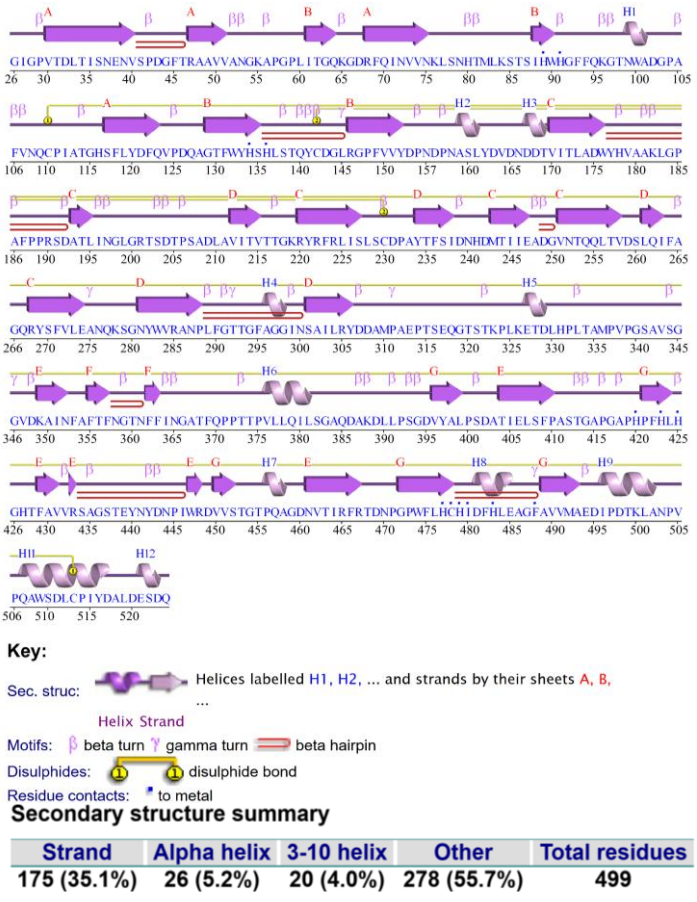

Figure 3 Secondary structure analysis using PDBSum

Tertiary Structure Prediction and Validation

Tertiary structure prediction of Thlacc1 was performed using homology modeling with Swiss Model, generating one model for each selected template, as detailed in Table 3. The templates were chosen based on the highest sequence similarity with *Thlacc1* laccase. The selected templates included 3pxl.1.A and 3fpx.1.A, both are laccases from *T. hirsuta*, and 5nq8.1.A, a laccase from *Trametes coccinea*. All predicted models were in a monomeric state.

Table 3 Preliminary structure validation of *Thlacc1* laccase based on homology modelling

Template and Seq Identity (%)	Generated Model	Structure Assessment: Ramachandran favored (%)	Model Coverage (%) and Number of Copper (Cu)
3pxl.1.A (77.87)	Model 01	96.57	99.56 and 3
5nq8.1.A (79.84)	Model 02	96.17	99.80 and 4
3fpx.1.A (77.96)	Model 03	96.58	100 and 4

Preliminary structure validation was conducted using the Structure Assessment tool. Among the generated models, Model 03, which was built using 3fpx.1.A as a template, provided the most accurate representation of the mature *Thlacc1* laccase. This model exhibited the highest Ramachandran favored percentage (96.58%) and had full model coverage (100%), along with the presence of four copper atoms. Structure validation of the selected models was performed by comparing each model with the template 3fpx.1.A, as this structure exhibited the highest similarity to *Thlacc1*. The results, summarized in Table 4, showed that Model 03 had a close match to the template in terms of ProSa (Z-score), ERRAT, Verify3D, and Qmean4 values. These findings confirmed that Model 03 was the most accurate representation of *Thlacc1* among the predicted models.

Table 4 Structure validation of *Thlacc1* laccase Model 03 vs template

Model	Structure Assessment: Ramachandran favored (%)	ProSa (Z-score)	ERRAT (%)	Verify 3D (%)	Qmean4
Model 03	96.78	-8.2	93.9709	91.58	1.15
3fpx.1.A	96.38	-8.06	93.6864	87.17	1.84

The superimposition of Model 03 with 3fpx.1.A further confirmed their structural similarity, with a root-mean-square deviation (RMSD) of 0.100 Å (Supplementary Figure S6). A detailed structural assessment of Model 03 is presented in Figure 4, where the Ramachandran plot (Figure 4b) indicates that most residues fall within the allowed or favorable regions. The normalized Qmean4 Z-score of 1.15 (Figure 4c) closely aligns with that of an experimental structure. The structural alignment between Model 03 and 3fpx.1.A (Figure 4d) highlights the confidence levels of each residue along the sequence. In contrast, the predicted local similarity analysis (Figure 4e) identifies regions with lower similarity to the template. Additionally, the ERRAT analysis (Supplementary Figure S7) identified three problematic regions, located around the 50th, 70th, and 390th residues, indicating local errors within Model 03. In summary, these findings demonstrate that Model 03 closely resembles the experimentally determined structure of a similar protein available in the protein database.

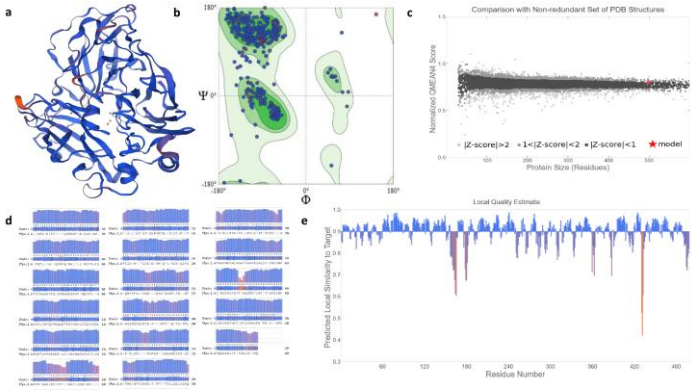

Figure 4 (a) Model 03 *Thlacc1* laccase, (b) Ramachandran plot of Model 03, (c) QMEAN structure result of Model 03 against Non redundant set of PDB structures,

(d) Alignment of Model 03 with 3fpx.1.A structure, (c) Predicted local similarity of the target with QMEANDisCo Global of 0.90 ± 0.05

Functional analysis of *Thlacc1* laccase

The InterProScan server identified the putative Thlacc1 laccase as a member of the Cupredoxin superfamily (IPR008972) and the Multicopper Oxidase family (IPR045087), containing three characteristic multicopper oxidase motifs: PF07732 (N-terminal Cu-oxidase), PF00394 (second Cu-oxidase), and PF07731 (C-terminal Cu-oxidase) (Supplementary Figure S8). This finding is further supported by the ProSite database, which identified a match to PS00079, a multicopper oxidase signature at residues 129–149: GtFwYhShLStqYcDGLrgpF. Additionally, the SignalP 6.0 server predicted a 25-residue signal peptide (SP) with a cleavage site between the 25th and 26th residues (Figure 5), suggesting the extracellular nature of the enzyme. As a result, the secreted protein consists of 499 residues, consistent with the tertiary structure predictions, which were all based on a 499-residue sequence.

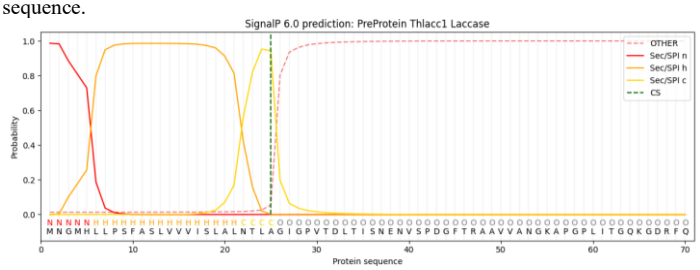

Figure 5 Signal peptide prediction of preprotein *Thlacc1* laccase with a likelihood of 0.9824 and a probability of 0.944272 cleavage site between residues 25 and 26

Functional analysis of glycosylation sites using NETNGLYC-1.0 and NETOGLYC-4.0 identified four potential N-glycosylation sites at residues 54-57 (NHTM), 133-136 (NASL), 333-336 (NGTN), and 436-439 (NVTI) (Supplementary Figure S9). Additionally, nine O-glycosylation sites were predicted at Ser178, Ser291, Thr295, Ser296, Thr297, Thr303, Thr309, Ser319, and Ser485. These findings suggest that the mature *Thlacc1* laccase may have a higher molecular weight than initially predicted if glycosylation occurs.

Multiple sequence alignment using the COBALT NCBI server successfully highlighted conserved (red) and non-conserved (blue) regions, four copper-binding domains, and conserved cysteine residues (yellow) (Supplementary Figure S10). The copper-binding domains of the secreted *Thlacc1* laccase were identified as follows: L1: residues 64-70 (HWHGFFQ), L2: residues 109-115 (HSHLSTQ), L3: residues 395-401 (HPFHLHG), and L4: residues 452-459 (HCHIDFHL). Five conserved cysteine residues were observed in the aligned sequences. In the mature *Thlacc1* laccase, these were located at C85, C117, C205, C453, and C488, indicating their structural and functional significance. Notably, C453 was situated within the L4 domain, directly interacting with a copper atom. This position was used to predict the laccase's redox potential by identifying the 10th residue after C453-F463 in this case, categorizing *Thlacc1* as a High-Redox Potential Laccase (HRPL) with a redox potential greater than 710 mV **(Mate and Alcalde, 2015)**. The remaining four conserved cysteine residues formed disulfide bonds: C117 paired with C205, while C85 bonded with C488, as shown in Figure 6. These disulfide bonds were conserved across all aligned sequences, reinforcing their importance in maintaining protein stability and function.

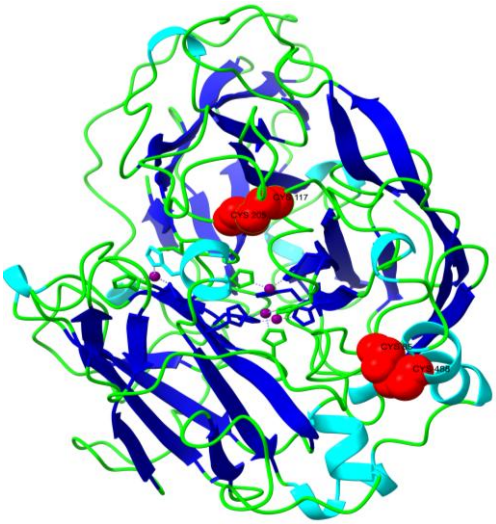

Figure 6 Solid ribbon representation of Model 03 *Thlacc1* laccase; α-helix (Cyan), β-sheet (Blue), coil (Green), copper atoms (purple), and disulfide bonds (Red, Sphere)

The temperature of melting (Tm) of the mature *Thlacc1* laccase was predicted to be 63.3 ºC using the SCOOP webserver (Supplementary Figure S11), suggesting that the enzyme exhibits good thermal stability. Substrate-binding cavity prediction was performed using the CB-Dock2 server, which identified a cavity centered near the L4 domain. Among the detected cavities, C6 (Figure 7) was selected for further analysis. This cavity was centered at x = 2, y = 18, z = 21 and had a volume of 221 Å³.

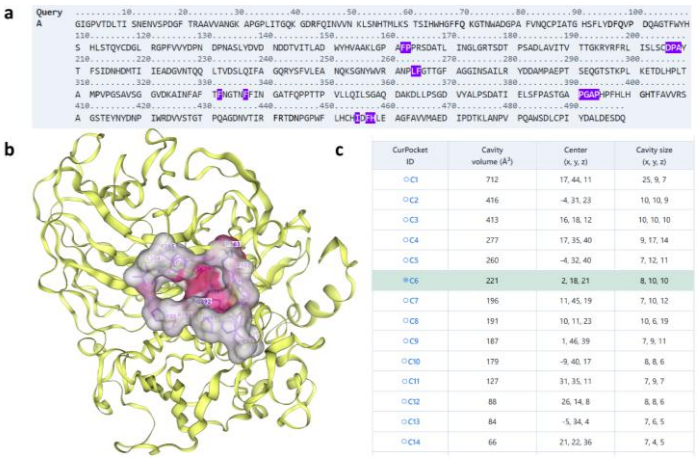

Figure 7 Substrate binding pocket analysis; (a) Highlighted amino acids involved in binding pocket formation, (b) Pocket of the catalytic site, (c) Number of cavities detected, highlighting pocket C6 as a potential catalytic pocket

Functional analysis of residues interacting with copper atoms was conducted to characterize their structural roles. As shown in Supplementary Figure S12, the analysis revealed the presence of a mononuclear copper center (Cu1-T1) and a trinuclear copper cluster (TNC), comprising Cu2-T2 and Cu3α, Cu3β-T3. The Cu1 was coordinated by His458, His395, and Cys453, while Cu2 by His398 and His64. Cu3α bonded to His111, His400, and His452, whereas Cu3β was coordinated by His109, His66, and His454.

Molecular Docking of *Thlacc1* Laccase to Synthetic Dyes

Docking analysis of 2,2′-azino-bis(3-ethylbenzothiazoline-6-sulfonic acid) (ABTS), the native substrate of laccase, was performed on the catalytic pocket of Model 03 to assess its binding interactions. Four residues were involved in interaction with ABTS through pi-pi stacking interactions (Phe265) and pi-alkyl interactions (Phe162, Phe337, and His458) (Supplementary Figure S13). These interactions resulted in a binding affinity of -6.316 kcal/mol, suggesting a stable docking pose. A previous study demonstrated that recombinant *Thlacc1* expressed in *Pichia pastoris* could oxidize ABTS up to 0.433788 U/mL in its crude form **(Ilham, 2025)**, confirming the enzyme's functionality.

To further investigate the bioremediation potential of *Thlacc1* laccase, docking simulations were performed with eight synthetic dyes using Model 03. Among the tested dyes, DB71 exhibited the highest binding affinity (-8.440 kcal/mol), followed by AB129 (-7.886 kcal/mol), AB113 (-7.838 kcal/mol), and RB4 (-7.773 kcal/mol). Other binding affinities included: RBBR (-6.611 kcal/mol), Anthraquinone (-6.488 kcal/mol), Indigosol (-6.278 kcal/mol), and RB5 (-5.825 kcal/mol) (Table 5). The specific interactions and interacting residues for each dye are detailed in Figure 8.

Table 5 Amino acids involved in contacts and binding energy in the molecular docking of laccase with synthetic dyes

Synthetic dyes	Residues in contact	Binding Energy (kcal mol^{-1})
Remazol Brilliant Blue R ($C_{22}H_{16}N_2Na_2O_{11}S_3$)	Pro164, Phe265, Gly392, Ala393	-6.611
Indigosol ($C_{18}H10C_{12}Na_2O_8S_4$)	Phe162, Phe265, Gly392, His458	-6.278
Anthraquinone ($C_{14}H_8O_2$)	Phe162, Phe265, Gly392, His458	-6.488
Acid Blue 129 ($C_{23}H_{19}N_2NaO_5S$)	Phe162, Phe265, Phe332, Gly334, Pro391, His458	-7.886
Acid Blue 113 ($C_{32}H_{21}N_5Na_2O_6S_2$)	Phe162, Leu264, Phe265, Phe332, Pro391	-7.838
Reactive Blue 4 ($C_{23}H_{14}Cl_2N_6O_8S_2$)	Phe162, Pro164, Phe265, Pro391, Gly392, Ala393, Pro431	-7.773
Reactive Black 5 ($C_{26}H_{21}N_5Na_4O_{19}S_6$)	Gln237, Phe239, Leu264, Gly392, Ser427, Gly429, Asp435, His458	-5.825
Direct Blue 71 ($C_{40}H_{23}N_7Na_4O_{13}S_4$)	Pro164, Leu264, Phe265, Pro394, Gly411, Asp435, His458	-8.440

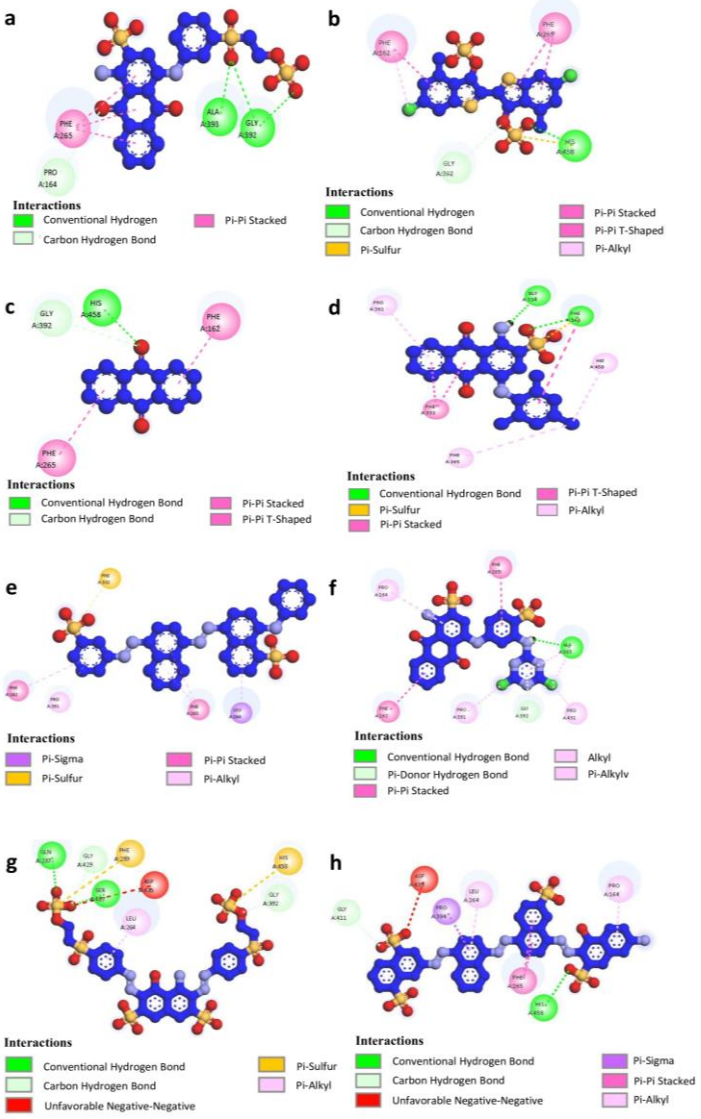

Figure 8 2D interactions of docking results against synthetic dyes; (a) Remazol Briliant Blue R ($C_{22}H_{16}N_2Na_2O_{11}S_3$), (b) Indigosol ($C_{18}H_{10}Cl_2Na_2O_8S_4$), (c) Anthraquinone ($C_{14}H_8O_2$), (d) Acid Blue 129 ($C_{23}H_{19}N_2NaO_5S$), (e) Acid Blue 113 ($C_{32}H_{21}N_5Na_2O_6S_2$), (f) Reactive Blue 4 ($C_{23}H_{14}Cl_2N_6O_8S_2$), (g) Reactive Black 5 ($C_{26}H_{21}N_5Na_4O_{19}S_6$), (h) Direct Blue 71 ($C_{40}H_{23}N_7Na_4O_{13}S_4$)

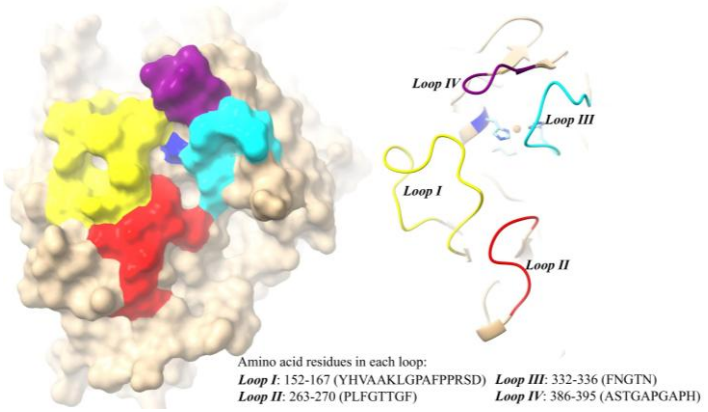

Figure 9 Loops around the catalytic pocket as potential hotspots for catalytic improvement via direct mutagenesis

Further analysis of binding localization successfully identified four key loops involved in dye interactions (Figure 9). *Loop I* (yellow) consists of 16 residues (152–167: YHVAAKLGPAFPPRSD), including Phe162, one of the most frequently interacting residues. *Loop II* (red) is composed of 8 residues (263–270: PLFGTTGF), where Phe265, another frequent interacting residue, is located. *Loop III* (cyan) is a short loop containing 5 residues (332–336: FNGTN), with Phe332 and Gly334 involved explicitly in interactions with AB129. *Loop IV* (purple) consists of 10 residues (386–395: ASTGAPGAPH), with Gly392 as a frequent interacting residue. These findings highlight the structural regions responsible for substrate recognition and binding, offering valuable insights into the dye degradation potential of *Thlacc1* laccase.

Experimental Validation of Decolorization Activity of Recombinant Thlacc1 Laccase to Synthetic Dyes

The results of the decolorization assays are presented in Figure 10, in which four selected dyes were evaluated using recombinant Thlacc1 laccase to examine whether binding affinity correlates positively with decolorization activity. The dyes were selected based on their binding affinity: Direct Blue 71 (DB71) represented the highest affinity, Acid Blue 113 (AB113) and Acid Blue 129 (AB129) represented moderate affinity, and Reactive Black 5 (RB5) represented the lowest affinity. The results indicate that binding affinity correlates with decolorization activity to some extent. DB71 and RB5 exhibited little to no decolorization (<2%) after 3 hours of incubation, whereas AB129 and AB113 showed decolorization efficiencies of 24.5% and 63.2%, respectively (Figure 10a), resulting in reduced color intensity, as shown in Figure 10b. These findings suggest that although binding affinity may positively influence the decolorization rate, other factors, such as molecular interactions and the specific amino acid residues involved at the enzyme's active site, may also play important roles in determining the decolorization efficiency of the tested dyes, as discussed in the previous analysis.

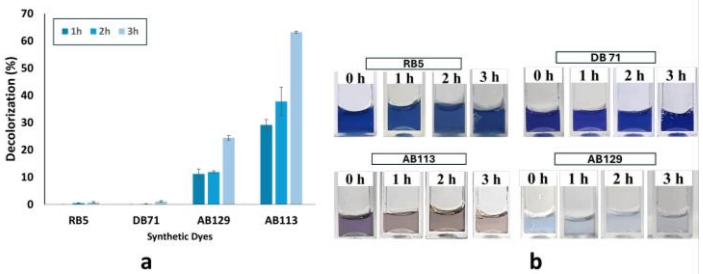

Figure 10 Decolorization assays result against selected dyes; (a) Decolorization rate at sampling points, (b) Color intensity at each incubation stage.

DISCUSSION

Laccases have low substrate specificities and low-toxicity byproducts, making them highly suitable for environmental applications. Recent research has focused on enhancing laccase production through screening new sources, recombinant production, and immobilization to improve its stability and reusability **(Dong *et al*., 2023)**. Despite its promising potential, efforts to obtain laccases suitable for large-scale applications remain a focus of research aimed at optimizing laccase's effectiveness and cost efficiency (**Strong and Claus, 2011**). *In silico* approaches provide valuable insights as a foundation for enhancing laccase efficiency through genetic engineering, thereby further improving its performance in terms of stability, selectivity, and catalytic activity for dye bioremediation processes**.**

In this study, a new laccase gene from *T. hirsuta* EDN 082, designated *Thlacc1*, was isolated using OPEFB as a gene inducer, further supporting the role of lignocellulosic sources in enhancing laccase gene transcription. The amino acid sequence of *Thlacc1* shows high protein sequence similarity of 98.47% to laccase 3 (*AOX15704.1*) and 98.09% to laccase 6 (*WDI23427.1*). Based on these results, *Thlacc1* laccase, laccase 3, and laccase 6 fall within the 2% threshold, suggesting that these are likely variants of the same gene rather than distinct genes (**Hall and Schwarz, 2015)**. Phylogenetic analysis further confirmed the close relationship among these genes, classifying them into the minor laccase group F based on orthology-based classification **(Savinova *et al.*, 2019)**. This classification suggests that they likely serve the same biological function in their respective organisms.

The amino acid sequence of *Thlacc1* laccase consisted of a substantial amount of non-polar residues (Supplementary Figure S4), such as Alanine (Ala), Valine (Val), Leucine (Leu), Isoleucine (Ile), and Phenylalanine (Phe). The binary patterns of polar and non-polar residues significantly influence the formation of regular secondary structures, with specific patterns favoring α-helices or β-strands **(Rebehmed *et al*., 2016)**. Non-polar residues like Val, Ile, Phe, and Cys promote β-strands, while Leu, Ala, and Met favor α-helices (Johansson *et al*., 2010) as shown in Supplementary Figure S5 and Figure 3. As macromolecular crowders, non-polar amino acids can stabilize proteins' native forms without substantially altering their secondary structure **(Pal and Mitra, 2022)**.

The predicted melting temperature of 63.3 °C suggests moderate thermal stability (Supplementary Figure S11) (Ebrahimi et al., 2011), although experimental validation is needed to confirm this property compared to the established thermostable laccase. Thermostable proteins exhibit higher frequencies of oppositely charged amino acids, particularly lysine and glutamic acid, which enhance electrostatic interactions **(Sun *et al*., 2020)**. Various structural adaptations also contribute to thermostability, including additional hydrogen bonds, salt bridges, and disulfide bonds **(Benrezkallah, 2024)**. In Supplementary Figure S11, five conserved cysteines were identified, four of which formed disulfide bonds as shown in Figure 6. The presence of these bonds correlated positively with the thermostability of the protein, as discussed earlier.

The physical characteristics of Thlacc1 laccase (Table 2), such as the aliphatic index, confirm the enzyme's thermostability. This characteristic is influenced by the presence of aliphatic amino acids, particularly alanine, isoleucine, leucine, proline, and valine. These residues play crucial roles in protein structure, engaging in hydrophobic interactions that stabilize secondary, tertiary, and quaternary structures **(AL Mughram *et al*., 2023)**. *Thlacc1* laccase has a molecular weight of 56,54 kDa, and pI of 4.88, which were similar to other laccases from group F of the same species **(Savinova *et al*., 2019)**. Instability index of 29.13 indicated that the *Thlacc1* laccase was stable in in vitro conditions **(Guruprasad *et al*., 1990)**, this result corresponded to previous study on crude laccase from *T. hirsuta* EDN 082, which showed that the enzyme retained 79.67 ± 4.92% of initial activity after 6 repeated cycles of uses, suggesting the good stability of the enzyme **(Anita *et al*., 2020)**. Grand average of hydropathicity of -0.130, indicating that the protein was hydrophilic **(Kyte and Doolittle, 1982),** meaning it has good solubility in water. The solubility of protein is crucial for large-scale production, as it facilitates the harvesting of protein from the production medium.

In Supplementary Figure S6, the tertiary structure of Model 03 is presented. This structure was obtained through homology modeling using the 3fpx.1. A structure as a template, a native laccase from *T. hirsuta* group A, which shares 77.96% sequence similarity with *Thlacc1* **(Polyakov *et al*., 2009)**. The 3fpx.1.A structure was selected due to the lack of an experimentally determined structure for group F laccases. Therefore, homology modeling using the closest available template was deemed more suitable for predicting the tertiary structure of *Thlacc1* laccase, as shown in Figure 4. The quality of Model 03 was further validated by a QMEAN4 Z-score of 1.15, indicating strong agreement with PDB structures of similar length **(Benkert *et al*., 2011)**.

The *Thlacc1* laccase was identified as part of the superfamily of oxidoreductases, within the family of multicopper oxidases (Figure S8), as supported by the detailed motifs. This family of enzymes contains one to six copper atoms per molecule, with a catalytic center comprising type I, II, and III copper domains, as shown in Supplementary Figure S12 **(Góralczyk-Bińkowska *et al*., 2019)**. This enzyme has signal peptides at residues 1-25 (Figure 5), which were crucial for protein secretion and translocation to the endoplasmic reticulum **(Owji *et al*., 2018; Dumitrescu *et al*., 2023)**. Therefore, identifying the signal peptide (SPs) is important before the gene target undergoes heterologous expression, as some native SPs were less effective in heterologous expression **(Pechsrichuang *et al*., 2016)**. The identified SP has a high likelihood of 0.9824 and a probability of 0.944272 of a cleavage site between residues 25 and 26. The presence of SP in laccase from *T. hirsuta* and other species within the *Trametes* genus was a shared motif; for example, all laccase genes from *T. hirsuta* registered in GeneBank have a signal peptide in their N-terminal. In the native organisms, laccases are secreted into the medium upon induction with lignocellulose or its derivatives **(Piscitelli *et al*., 2011)**, as shown in this study with OPFEB.

Glycosylation, both N-linked and O-linked, is an important post-translational modification of the protein. The *Thlacc1* laccase contained four glycosylation sites. N-glycosylation sites are typically characterized by the presence of the consensus sequence Asn-Xaa-Ser/Thr or N-X-S/T (where X ≠ Pro) **(Lowenthal *et al*., 2016)**. Glycosylated asparagines are located in loop regions within the protein's 2D structure **(Lam *et al*., 2013)**. In comparison, nine O-Glycosylation sites were predicted. O-glycosylation is more commonly observed in recombinant proteins expressed under methanol induction **(Radoman *et al*., 2021)**. The O-glycan chains typically consist of short mannose residues, including mannose with α-1,2-, α-1,3-, and α-1,6-linkages **(Boraston *et al*., 2003)**. The combination of N- and O-glycosylation can account for 10-30% of the molecular mass of laccase **(Maestre-Reyna *et al*., 2015)**, suggesting that the secreted *Thlacc1* laccase may have a higher molecular weight than predicted (>56.54 kDa), if expressed in a heterologous host such as *P. pastoris*.

Multiple sequence alignment of laccases revealed the conserved copper-binding regions: HWHGFFQ, HSHLSTQ, HPFHLHG, and HCHIDFHL. These sequences align with the copper-binding motifs previously reported by **Pereira-Patrón *et al.* (2019)**. The L1 and L2 motifs are located near the N-terminal, while L3 and L4 are positioned closer to the C-terminal of *Thlacc1* laccase. Additionally, the sequence HCHIDFHLEAGF, a hallmark of high-redox-potential laccases initially identified in *T. hirsuta* laccases by **Mate and Alcalde (2015)**, was also found in *Thlacc1* from *T. hirsuta* EDN 082. The L4 domain is situated around the T1 copper atom, where the predicted catalytic pocket is located (Figure 7). This catalytic pocket contains the H458 residue, which is directly in contact with T1. In Model 03, the T1 copper atom is connected to the trinuclear copper (TNC) cluster through the T1-Cys543-His452-T3 pathway (Supplementary Figure S12), a configuration similar to that reported by **Augustine *et al.* (2008)**. The T1 copper atom plays a crucial role in substrate oxidation and electron transfer to the TNC cluster. At the same time, the TNC complex reduces molecular oxygen to water by utilizing the redox potential difference between the substrate at T1 and the TNC cluster **(Jones and Solomon, 2015)**.

The use of laccase as a green catalyst has gained significant interest in recent years, particularly for the bioremediation of synthetic dyes. In this study, we investigated the potential of Thlacc1 laccase as a catalyst for the decolorization of synthetic dyes. Docking analysis was conducted on eight different dyes, revealing multiple interacting residues (Figure 8) and their respective binding affinities (Table 6), followed by experimental validation using four selected dyes (Figure 10). Molecular docking results suggest a potential binding affinity with synthetic dyes, where RBBR, Indigosol, Anthraquinone, and AB129 formed interactions with specific residues, as observed in Model 03, compared to ABTS, which exhibited comparable binding affinities. This suggests that *Thlacc1* laccase may be capable of effectively oxidizing these dyes. Previous studies on crude laccase from *T. hirsuta* EDN 082 demonstrated significant bioremediation potential for Remazol Brilliant Blue R, anthraquinone, and azo dyes **(Anita *et al*., 2020; Yanto *et al*., 2022)**. Direct Blue 71 (DB71) exhibited the highest predicted binding affinity (-8.44 kcal/mol), suggesting potential decolorization activity. However, experimental validation contradicted this prediction, as DB71 showed only 1.1% decolorization after 3 h of incubation. In contrast, the decolorization rates of the other tested dyes appeared to correlate positively with their predicted binding affinities. The recombinant Thlacc1 laccase was unable to decolorize Reactive Black 5 (RB5; <1%), consistent with previous findings reported by **Yanto *et al.* (2022).** Meanwhile, Acid Blue 113 (AB113) and Acid Blue 129 (AB129) were successfully decolorized by recombinant Thlacc1 laccase, albeit at different rates (63.2% and 24.5%, respectively). These results suggest that factors beyond binding affinity play a crucial role in determining the efficiency of dye decolorization. Molecular interaction analysis revealed that Phe162, Phe265, Gly392, and His458 were the most frequently interacting residues, suggesting their potential involvement in substrate oxidation. Notably, Phe162 formed interactions with all positively tested substrates, namely ABTS, AB113, and AB129. The absence of interactions with Phe162 may explain the lack of decolorization observed for DB71 and RB5, despite both having the highest and lowest binding affinities, respectively. Structural analysis further showed that the aromatic ring of Phe162 protrudes inward due to its nonpolar nature and is positioned in proximity to His458, which coordinates the T1 catalytic copper site. This may help to coordinate and stabilize the substrate into the catalytic site. Overall, our findings suggest that a combination of binding affinity and appropriate interactions with key active-site residues, such as Phe162, governs the effectiveness of dye decolorization by laccase.

The binding localization analysis on *Loop I-IV* (Figure 9) indicated that the presence of Phenilalanin (Phe) and Gycine (Gly) in the loops was important for ligand binding to *Thlacc1* laccase. The loops could potentially become hotspots for improving protein-ligand interactions through genetic engineering. A similar approach by **Zhan *et al.* (2022)** successfully identified residues within the loop

structure of the catalytic pocket of a laccase, and site-directed mutagenesis targeting these residues enhanced the decolorization of synthetic dyes. Therefore, identifying potential residues is crucial for future studies. This *in silico* analysis, followed by experimental validation, provides structural and functional insights; however, a more thorough investigation is still needed to reveal the decolorization potential of Thlacc1 against more diverse types of dyes.

CONCLUSION

This study successfully presented detailed steps for exploring the laccase gene from a species of white-rot fungus, T. hirsuta EDN 082, by combining classical primer design, PCR, and sequencing. Two potential laccase-encoding genes were successfully identified and subsequently classified as a single gene (*Thlacc1*). Gene characterization revealed that the *Thlacc1* gene belongs to the minor laccase group F, based on its phylogenetic analysis, and encodes an extracellular blue laccase with a high redox potential. Physical analysis revealed that *Thlacc1* laccase has a molecular weight of 56.54 kDa and is a soluble globular enzyme with an acidic nature. It is also classified as a thermostable protein based on its predicted melting temperature.

Structural analysis revealed the secondary structure of the protein, providing valuable insights into the structural organization of the *Thlacc1* protein. Tertiary structure predictions presented a reliable model based on structural assessment, as well as the methods used in prediction. The functional analysis presented motifs unique to multicopper oxidases, conserved residues involved in copper binding and catalytic pocket formation, disulfide bonds, predictions for N-linked and O-linked glycosylation, and the catalytic domain of the protein. Molecular docking revealed that *Thlacc1* laccase has potential as a catalyst for the bioremediation of multiple synthetic dyes, based on its binding affinity and interactions with residues within the identified loops surrounding the catalytic pocket. Meanwhile, experimental validation confirmed the ability of Thlacc1 laccase to decolorize dyes and that the combination of binding affinity and interacting residues plays a crucial role in determining the decolorization efficiency of dyes.

Catalytic efficiency may also be improved through genetic engineering that targets the residues within the loops. Although the potential of *Thlacc1* laccase is immense, a more thorough experimental validation remains necessary to better understand its future applications in decolorization.

Acknowledgments: Muhamad Ilham gratefully acknowledges the Master's scholarship from LPDP (the Indonesian Endowment Fund for Education, Ministry of Finance, Republic of Indonesia).

REFERENCES

Agrawal, K., & Verma, P. (2020). Multicopper oxidase laccases with distinguished spectral properties: A new outlook. *Heliyon, 6(5)*, e03972. https://doi.org/10.1016/j.heliyon.2020.e03972

AL Mughram, M. H., Catalano, C., Herrington, N. B., Safo, M. K., & Kellogg, G. E. (2023). 3D interaction homology: The hydrophobic residues alanine, isoleucine, leucine, proline, and valine play different structural roles in soluble and membrane proteins. *Front Mol Biosci, 10*, 2023. https://doi.org/10.3389/fmolb.2023.1116868

Al-Tohamy, R., Ali, S. S., Li, F., Okasha, K. M., Mahmoud, Y. A., Elsamahy, T., Jiao, H., Fu, Y., & Sun, J. (2022). A critical review on the treatment of dye-containing wastewater: Ecotoxicological and health concerns of textile dyes and possible remediation approaches for environmental safety. *Ecotoxicol Environ Saf, 231*, 113160. https://doi.org/10.1016/j.ecoenv.2021.113160

Anita, S., Ardiati, F., Oktaviani, M., Sari, F., Dwi, N. O., Ramadhan, K., & Yanto, D. (2020). Immobilization of laccase from *Trametes hirsuta* EDN 082 in light expanded clay aggregate for decolorization of Remazol Brilliant Blue R dye. *Bioresour Technol Rep, 12*, 100602. https://doi.org/10.1016/j.biteb.2020.100602

Augustine, A. J., Kragh, M. E., Sarangi, R., Fujii, S., Liboiron, B. D., Stoj, C. S., Kosman, D. J., Hodgson, K. O., Hedman, B., & Solomon, E. I. (2008). Spectroscopic studies of perturbed T1 Cu sites in the multicopper oxidases *Saccharomyces cerevisiae* Fet3p and *Rhus vernicifera* laccase: Allosteric coupling between the T1 and trinuclear Cu sites. *Biochemistry, 47(7)*, 2036-2045. https://doi.org/10.1021/bi7020052

Barrios-Estrada, C., de Jesús Rostro-Alanis, M., Parra, A. L., Belleville, M. P., Sanchez-Marcano, J., Iqbal, H. M., & Parra-Saldívar, R. (2018). Potentialities of active membranes with immobilized laccase for bisphenol A degradation. *Int J Biol Macromol, 108*, 837–844. https://doi.org/10.1016/j.ijbiomac.2017.10.177

Benkert, P., Biasini, M., & Schwede, T. (2011). Toward the estimation of the absolute quality of individual protein structure models. *Bioinformatics, 27(3)*, 343–350. https://doi.org/10.1093/bioinformatics/btq662

Benrezkallah, D. (2024). Molecular dynamics simulations at high temperatures of the *Aeropyrum pernix* L7Ae thermostable protein: Insight into the unfolding pathway. *J Mol Graph Model, 127*, 108700. https://doi.org/10.1016/j.jmgm.2023.108700

Boraston, A. B., Sandercock, L., Warren, R. A., & Kilburn, D. G. (2003). O-glycosylation of a recombinant carbohydrate-binding module mutant secreted by *Pichia pastoris*. *J Mol Microbiol Biotechnol, 5(1)*, 29-36. https://doi.org/10.1159/000068721

Cardullo, N., Muccilli, V., & Tringali, C. (2022). Laccase-mediated synthesis of bioactive natural products and their analogues. *RSC Chem Biol, 3(6)*, 614-647. https://doi.org/10.1039/d1cb00259g

Chen, Z., & Duan, X. (2011). Ribosomal RNA depletion for massively parallel bacterial RNA-sequencing applications. *Methods Mol Biol, 733*, 93–103. https://doi.org/10.1007/978-1-61779-089-8_7

Damborsky, J., & Brezovsky, J. (2014). Computational tools for designing and engineering enzymes. *Curr Opin Chem Biol, 19*, 8–16. https://doi.org/10.1016/j.cbpa.2013.12.003

Das, S., Cherwoo, L., & Singh, R. (2023). Decoding dye degradation: Microbial remediation of textile industry effluents. *Biotechnol Notes, 4*, 64–76. https://doi.org/10.1016/j.biotno.2023.10.001

Dong, C. D., Tiwari, A., Anisha, G. S., Chen, C. W., Singh, A., Haldar, D., Patel, A. K., & Singhania, R. R. (2023). Laccase: A potential biocatalyst for pollutant degradation. *Environ Pollut, 319*, 120999. https://doi.org/10.1016/j.envpol.2023.120999

Dumitrescu, A., Jokinen, E., Paatero, A., Kellosalo, J., Paavilainen, V. O., & Lähdesmäki, H. (2023). TSignal: A transformer model for signal peptide prediction. *Bioinformatics, 39(Suppl 1)*, i347–i356. https://doi.org/10.1093/bioinformatics/btad228

Dutta, B., Banerjee, A., Chakraborty, P., & Bandopadhyay, R. (2018). *In silico* studies on bacterial xylanase enzyme: Structural and functional insight. *J Genet Eng Biotechnol, 16(2)*, 749-756. https://doi.org/10.1016/j.jgeb.2018.05.003

Ebert, M. C., & Pelletier, J. N. (2017). Computational tools for enzyme improvement: Why everyone can—and should—use them. *Curr Opin Chem Biol, 37*, 89–96. https://doi.org/10.1016/j.cbpa.2017.01.021

Ebrahimi, M., Lakizadeh, A., Agha-Golzadeh, P., Ebrahimie, E., & Ebrahimi, M. (2011). Prediction of thermostability from amino acid attributes by combination of clustering with attribute weighting: A new vista in engineering enzymes. *PLoS One, 6(8)*, e23146. https://doi.org/10.1371/journal.pone.0023146

Farnet, A. M., Criquet, S., Tagger, S., Gil, G., & Le, P. J. (2000). Purification, partial characterization and reactivity with aromatic compounds of two laccases from *Marasmius quercophillus* strain 17. *J Microbiol, 46*, 189–194. https://doi.org/10.1139/cjm-46-3-189

Forootanfar, H., Moezzi, A., Aghaie-Khozani, M., Mahmoudjanlou, Y., Ameri, A., Niknejad, F., & Faramarzi, M. A. (2012). Synthetic dye decolorization by three sources of fungal laccase. *Iran J Environ Health Sci Eng, 9(1)*, 27. https://doi.org/10.1186/1735-2746-9-27

Giardina, P., Faraco, V., Pezzella, C., Piscitelli, A., Vanhulle, S., & Sannia, G. (2010). Laccases: A never-ending story. *Cell Mol Life Sci, 67(3)*, 369-385. https://doi.org/10.1007/s00018-009-0169-1

Góralczyk-Bińkowska, A., Jasińska, A., & Długoński, J. (2019). Characteristics and use of multicopper oxidases enzymes. *Adv Microbiol, 58(1)*, 7–18. https://doi.org/10.21307/PM-2019.58.1.007

Guruprasad, K., Reddy, B. V., & Pandit, M. W. (1990). Correlation between stability of a protein and its dipeptide composition: A novel approach for predicting *in vivo* stability of a protein from its primary sequence. *Protein Eng, 4(2)*, 155-161. https://doi.org/10.1093/protein/4.2.155

Hall, R. M., & Schwarz, S. (2016). Resistance gene naming and numbering: Is it a new gene or not? *J Antimicrob Chemother, 71(3)*, 569–571. https://doi.org/10.1093/jac/dkv351

Hall, T. A. (1999). BioEdit: A user-friendly biological sequence alignment editor and analysis program for Windows 95/98/NT. *Nucl Acids Symp Ser, 41*, 95-98.

Holkar, C. R., Jadhav, A. J., Pinjari, D. V., Mahamuni, N. M., & Pandit, A. B. (2016). A critical review on textile wastewater treatments: Possible approaches. *J Environ Manag, 182*, 351–366. https://doi.org/10.1016/j.jenvman.2016.07.090

Hoque, M. B., Oyshi, T. H., Hannan, M. A., Haque, P., Rahman, M. M., Shahid, M. A., & Sheikh, S. (2024). Unraveling the ecological footprint of textile dyes: A growing environmental concern. *Pollut Stud, 5(2)*, 3014. https://doi.org/10.54517/ps.v5i2.3014

Ilham, M. (2025). Isolation, characterization, and heterologous expression of laccase-encoding gene from *Trametes hirsuta* EDN 082 in *Pichia pastoris*. *Thesis, IPB University*.

Jain, A. (2020). *Basic techniques in biochemistry, microbiology and molecular biology: Principles and techniques*. Springer Protocols Handbooks. https://doi.org/10.1007/978-1-4939-9861-6_25

Johansson, J., Nerelius, C., Willander, H., & Presto, J. (2010). Conformational preferences of non-polar amino acid residues: An additional factor in amyloid formation. *Biochem Biophys Res Commun, 402(3)*, 515-518. https://doi.org/10.1016/j.bbrc.2010.10.062

Jones, S. M., & Solomon, E. I. (2015). Electron transfer and reaction mechanism of laccases. *Cell Mol Life Sci, 72(5)*, 869–883. https://doi.org/10.1007/s00018-014-1826-6

Jorge, A. M. S., Athira, K. K., Alves, M. B., Gardas, R. L., & Pereira, J. F. B. (2023). Textile dye effluents: Current scenarios and the use of aqueous biphasic systems for dye recovery. *J Water Process Eng, 55*, 104125. https://doi.org/10.1016/j.jwpe.2023.104125

Kim, C., Lorenz, W. W., Hoopes, J. T., & Dean, J. F. (2001). Oxidation of phenolate siderophores by the multicopper oxidase encoded by the *Escherichia*

coli yacK gene. *J Bacteriol, 183*, 4866–4875. https://doi.org/10.1128/JB.183.16.4866-4875.2001
Kumar, S., Stecher, G., Li, M., Knyaz, C., & Tamura, K. (2018). MEGA X: Molecular Evolutionary Genetics Analysis across computing platforms. *Mol Biol Evol, 35(6)*, 1547-1549. https://doi.org/10.1093/molbev/msy096
Kyte, J., & Doolittle, R. F. (1982). A simple method for displaying the hydropathic character of a protein. *J Mol Biol, 157(1)*, 105-132. https://doi.org/10.1016/0022-2836(82)90515-0
Lam, P. V., Goldman, R., Karagiannis, K., Narsule, T., Simonyan, V., Soika, V., & Mazumder, R. (2013). Structure-based comparative analysis and prediction of N-linked glycosylation sites in evolutionarily distant eukaryotes. *Genomics Proteomics Bioinformatics, 11(2)*, 96–104. https://doi.org/10.1016/j.gpb.2012.11.003
Li, K., Shrivastava, S., & Stockwell, T. B. (2015). Degenerate primer design for highly variable genomes. *Methods Mol Biol, 1275*, 103–115. https://doi.org/10.1007/978-1-4939-2365-6_7
Lowenthal, M. S., Davis, K. S., Formolo, T., Kilpatrick, L. E., & Phinney, K. W. (2016). Identification of novel N-glycosylation sites at noncanonical protein consensus motifs. *J Proteome Res, 15(7)*, 2087–2101. https://doi.org/10.1021/acs.jproteome.5b00733
Maestre-Reyna, M., Liu, W. C., Jeng, W. Y., Lee, C. C., Hsu, C. A., Wen, T. N., Wang, A. H. J., & Shyur, L. F. (2015). Structural and functional roles of glycosylation in fungal laccase from *Lentinus* sp. *PLoS One, 10*, e0120601. https://doi.org/10.1371/journal.pone.0120601
Magdeldin, S., Yoshida, Y., Li, H., Maeda, Y., Yokoyama, M., Enany, S., Zhang, Y., Xu, B., Fujinaka, H., Yaoita, E., Sasaki, S., & Yamamoto, T. (2012). Murine colon proteome and characterization of the protein pathways. *BioData Min, 5(1)*, 11. https://doi.org/10.1186/1756-0381-5-11
Marco-Urrea, E., Pérez-Trujillo, M., Blánquez, P., Vicent, T., & Caminal, G. (2010). Biodegradation of the analgesic naproxen by *Trametes versicolor* and identification of intermediates using HPLC-DAD-MS and NMR. *Bioresour Technol, 101(7)*, 2159–2166. https://doi.org/10.1016/j.biortech.2009.11.019
Mate, D. M., & Alcalde, M. (2015). Laccase engineering: From rational design to directed evolution. *Biotechnol Adv, 33(1)*, 25–40. https://doi.org/10.1016/j.biotechadv.2014.12.007
Meng, E. C., Goddard, T. D., Pettersen, E. F., Couch, G. S., Pearson, Z. J., Morris, J. H., & Ferrin, T. E. (2023). UCSF ChimeraX: Tools for structure building and analysis. *Protein Sci, 32(11)*, e4792. https://doi.org/10.1002/pro.4792
Morozova, O. V., Shumakovich, G. P., Shleev, S. V., & Yaropolov, Y. I. (2007). Laccase-mediator systems and their applications: A review. *Appl Biochem Microbiol, 43*, 523-535. PMID: 18038679
Nene, T., Yadav, M., & Yadav, H. S. (2022). Plant catalase *in silico* characterization and phylogenetic analysis with structural modeling. *J Genet Eng Biotechnol, 20(1)*, 125. https://doi.org/10.1186/s43141-022-00404-6
Owji, H., Nezafat, N., Negahdaripour, M., Hajiebrahimi, A., & Ghasemi, Y. (2018). A comprehensive review of signal peptides: Structure, roles, and applications. *Eur J Cell Biol, 97(6)*, 422–441. https://doi.org/10.1016/j.ejcb.2018.06.003
Pal, S., & Mitra, R. K. (2022). Investigation on the effect of nonpolar amino acids as macromolecular crowders on the stability of globular proteins. *Chem Thermodyn Therm Anal, 6*, 100044. https://doi.org/10.1016/j.ctta.2022.100044
Panwar, P., Mahajan, P., & Kaushal, J. (2023). Microbial bioremediation of azo dyes: An environmentally sustainable technology. *Remediation.* https://doi.org/10.1002/rem.21745
Pechsrichuang, P., Songsiriritthigul, C., Haltrich, D., Roytrakul, S., Namvijtr, P., Bonaparte, N., & Yamabhai, M. (2016). OmpA signal peptide leads to heterogeneous secretion of *B. subtilis* chitosanase enzyme from *E. coli* expression system. *SpringerPlus, 5(1)*, 1200. https://doi.org/10.1186/s40064-016-2893-y
Pereira-Patrón, A., Solis-Pereira, S., Lizama-Uc, G., Ramírez-Prado, J. H., Pérez-Brito, D., & Tapia-Tussell, R. (2019). Molecular characterization of laccase genes from the basidiomycete *Trametes hirsuta* Bm-2 and analysis of the 5' untranslated region (5'UTR). *3 Biotech, 9(4)*, 160. https://doi.org/10.1007/s13205-019-1691-y
Piscitelli, A., Del Vecchio, C., Faraco, V., Giardina, P., Macellaro, G., Miele, A., Pezzella, C., & Sannia, G. (2011). Fungal laccases: Versatile tools for lignocellulose transformation. *C R Biol, 334(11)*, 789–794. https://doi.org/10.1016/j.crvi.2011.06.007
Polyakov, K. M., Fedorova, T. V., Stepanova, E. V., Cherkashin, E. A., Kurzeev, S. A., Strokopytov, B. V., Lamzin, V. S., & Koroleva, O. V. (2009). Structure of native laccase from *Coriolus hirsutus* at 1.8 Å resolution. Retrieved from https://www.rcsb.org/structure/3FPX
Pozdnyakova, N. N., Turkovskaya, O. V., Yudina, E. N., & Rodakiewicz-Nowak, Y. (2006). Yellow laccase from the fungus *Pleurotus ostreatus* D1: Purification and characterization. *Appl Biochem Microbiol, 42*, 56–61. https://doi.org/10.1134/S000368380601008X
Radoman, B., Grünwald-Gruber, C., Schmelzer, B., Zavec, D., Gasser, B., Altmann, F., & Mattanovich, D. (2021). The degree and length of O-glycosylation of recombinant proteins produced in *Pichia pastoris* depends on the nature of the protein and the process type. *Biotechnol J, 16(3)*, e2000266. https://doi.org/10.1002/biot.202000266
Rebehmed, J., Quintus, F., Mornon, J. P., & Callebaut, I. (2016). The respective roles of polar/nonpolar binary patterns and amino acid composition in protein regular secondary structures explored exhaustively using hydrophobic cluster analysis. *Proteins, 84(5)*, 624-638. https://doi.org/10.1002/prot.25012
Savinova, O. S., Moiseenko, K. V., Vavilova, E. A., Chulkin, A. M., Fedorova, T. V., Tyazhelova, T. V., & Vasina, D. V. (2019). Evolutionary relationships between the laccase genes of *Polyporales*: Orthology-based classification of laccase isozymes and functional insight from *Trametes hirsuta*. *Front Microbiol, 10*, 152. https://doi.org/10.3389/fmicb.2019.00152
Sondhi, S., Chopra, N. K., Kumar, A., & Gupta, N. (2023). Laccase: A green solution for environmental problems. *Adv Environ Eng Res, 4(2)*, 030. https://doi.org/10.21926/aeer.2302030
Strong, P. J., & Claus, H. (2011). Laccase: A review of its past and its future in bioremediation. *Crit Rev Environ Sci Technol, 41(4)*, 373–434. https://doi.org/10.1080/10643380902945706
Sudarshan, S., Harikrishnan, S., RathiBhuvaneswari, G., Alamelu, V., Aanand, S., Rajasekar, A., & Govarthanan, M. (2022). Impact of textile dyes on human health and bioremediation of textile industry effluent using microorganisms: Current status and future prospects. *J Appl Microbiol, 134*, 1–23. https://doi.org/10.1093/jambio/lxac064
Sun, S., Ao, C., Wang, D., & Dong, B. (2020). The frequencies of oppositely charged, uncharged polar, and β-branched amino acids determine proteins' thermostability. *IEEE Access, 8*, 66839–66845. https://doi.org/10.1109/ACCESS.2020.2985737
Vasina, D. V., Pavlov, A. R., & Koroleva, O. V. (2016). Extracellular proteins of *Trametes hirsuta* st. 072 induced by copper ions and a lignocellulose substrate. *BMC Microbiol, 16*, 106. https://doi.org/10.1186/s12866-016-0729-0
Viswanath, B., Rajesh, B., Janardhan, A., Kumar, A. P., & Narasimha, G. (2014). Fungal laccases and their applications in bioremediation. *Enzyme Res, 2014*, 163242. https://doi.org/10.1155/2014/163242
Yanto, D. H. Y., Anita, S. H., & Solihat, N. N. (2022). Enzymatic degradation and metabolic pathway of acid blue 129 dye by crude laccase from newly isolated *Trametes hirsuta* EDN 082. *Biocatal Biotransfor.* https://doi.org/10.1080/10242422.2022.2138360
Yanto, D. H. Y., Auliana, N., Anita, S., & Watanabe, T. (2019). Decolorization of synthetic textile dyes by laccase from newly isolated *Trametes hirsuta* EDN084 mediated by violuric acid. *IOP Conference Series: Earth and Environmental Science, 374*, 012005. https://doi.org/10.1088/1755-1315/374/1/012005
Yanto, D. H. Y., Guntoro, M. A., Nurhayat, O. D., Anita, S. H., Oktaviani, M., Ramadhan, K. P., Pradipta, M. F., & Watanabe, T. (2021). Biodegradation and biodetoxification of batik dye wastewater by laccase from *Trametes hirsuta* EDN 082 immobilised on light expanded clay aggregate. *3 Biotech, 11(5)*, 247. https://doi.org/10.1007/s13205-021-02806-8
Yaseen, D. A., & Scholz, M. (2019). Textile dye wastewater characteristics and constituents of synthetic effluents: A critical review. *Int J Environ Sci Technol, 16*, 1193–1226. https://doi.org/10.1007/s13762-018-2130-z
Zhan, J., Sun, H., Dai, Z., Zhang, Y., & Yang, X. (2022). Loops constructing the substrate-binding site controlled the catalytic efficiency of *Thermus thermophilus* SG0.5JP17-16 laccase. *Biochimie, 200*, 60–67. https://doi.org/10.1016/j.biochi.2022.05.010
Zhao, J., Mou, Y., Shan, T., Li, Y., Zhou, L., Wang, M., & Wang, J. (2010). Antimicrobial metabolites from the endophytic fungus *Pichia guilliermondii* isolated from *Paris polyphylla* var. *yunnanensis*. *Molecules, 15*, 7961–7970. https://doi.org/10.3390/molecules15117961